Tracking and Robustness Analysis for Controlled Microelectromechanical Relays

Michael Malisoff* Frédéric Mazenc† Marcio de Queiroz‡

Abstract

The feedback control problem for microelectromechanical (MEM) relays is complicated by a quadratic nonlinearity in the dynamic model. We show that this nonlinearity imposes constraints on the reference trajectories that can be tracked, and on the global convergence rate of the tracking error. Using a dynamic model that is applicable to both electrostatic and electromagnetic MEM relays, we introduce a new class of nonlinear tracking controls. In particular, we use Lyapunov theory to construct a state feedback that yields uniform global asymptotic stability and arbitrarily fast local exponential convergence of the tracking error. We then show how our control can be redesigned with partial-state feedback under the assumption that only the movable electrode position and the electrical state (i.e., charge or flux) are fed back. Finally, we utilize input-to-state stability theory to quantify the robustness of our state feedback controller to parametric uncertainties. Our simulation results illustrate the good stability and tracking performance of the proposed control. They also illustrate how to craft a reference trajectory that satisfies the aforementioned constraints while being compatible with a typical relay operation.

Key Words: MEM relays, nonlinear control, Lyapunov theory, input-to-state stability, observer

1 Introduction

Relays are used in a variety of industrial applications to open or close the connection in an electric circuit. Traditional mechanical relays, although large, slow, and noisy, are still widely used in various industrial control processes. Solid-state relays have much longer lifetimes, faster response, and smaller sizes than mechanical relays. However, solid-state relays have low off-resistance and high on-resistance, resulting in high-power consumption and poor electrical isolation. Design trade-offs for reducing their on-resistance tend to increase output

*Department of Mathematics, Louisiana State University, Baton Rouge, LA 70803-4918, malisoff@lsu.edu. Supported by NSF/DMS Grant 0424011.

†Projet MERE INRIA-INRA, UMR Analyse des Systèmes et Biométrie INRA, 2 pl. Viala, 34060 Montpellier, France, Frederic.Mazenc@supagro.inra.fr. Some of this work was carried out while this author visited Louisiana State University. He appreciates the kind hospitality he enjoyed during this period.

‡Department of Mechanical Engineering, Louisiana State University, Baton Rouge, LA 70803-6413, dequeiroz@me.lsu.edu. Supported by NSF/DMS Grant 0424011 and NSF/CAREER Grant 0447576.

capacitance, which introduces additional problems in applications involving the switching of high-frequency signals [18].

Microelectromechanical systems (MEMS) technology has created opportunities for developing new types of signal and power relays [18]. Compared with solid-state relays, MEM relays have the same advantages as mechanical relays, viz., lower on-resistance, higher off-resistance, higher dielectric strength, lower power consumption, and lower cost. In addition, by using MEMS technology to miniaturize mechanical relays, the problems of size and switching time are treated. Finally, micro-relays can be readily integrated with other electronic components.

MEM relays are generally split into two categories based on their method of actuation: electrostatic and electromagnetic [4, 5, 6, 7, 14, 18]. Relays consist of two circuits, a control circuit and an output circuit. In electrostatic relays, both circuits share a pair of parallel electrodes (one movable and one fixed) that act as a capacitor; see Figure 1 below. A voltage applied across the two electrodes generates an electric field between them, which in turn creates an attractive force between the electrodes. Once the electrodes come together, the two contacts of the output circuit also come together, allowing for the flow of current and closing the circuit. In electromagnetic relays, the control circuit consists of an electromagnet whose magnetic force acts on a movable electrode situated above the fixed coil post; again see Figure 1. The magnetic force attracts the electrode and closes the output circuit in the same manner as the electrostatic relay.

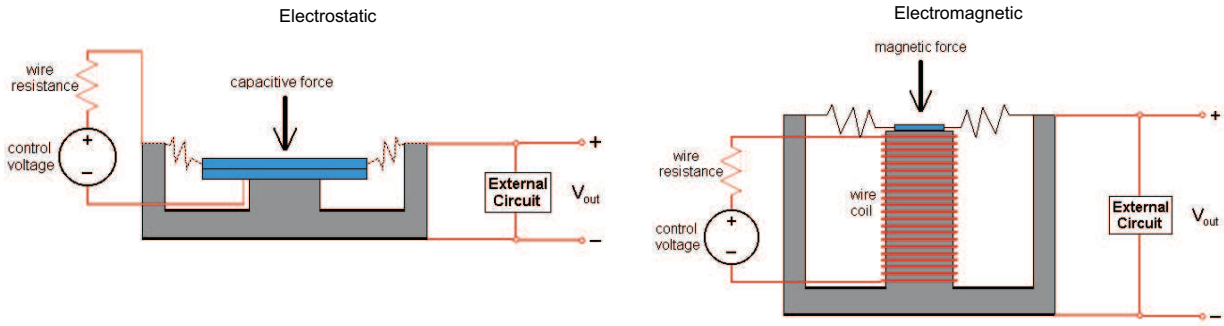

Figure 1: MEM Relays Model

The more common actuation method for micro-relays is electrostatic [18]. This is mostly due to difficulties in fabricating micro-size electromagnetic actuators. Another disadvantage is that electromagnetic actuation requires larger current, which leads to larger power consumption and larger heat generation. Nevertheless, [4] examines both actuation methods in their ability to achieve micron and submicron precision in rapid motion, and concludes that there is a strong case to be made in favor of magnetically-driven micro-actuators. See [7, 18] for a more detailed literature review on the design and fabrication of electrostatic and electromagnetic micro-relays.

Voltage-controlled MEM actuators exhibit an important nonlinear phenomenon called *pull-in* [15]. Mathematically, pull-in is associated with a saddle-node bifurcation [10]. Pull-in can be physically explained as follows. Suppose that the voltage across the MEM actuator is incrementally increased from zero. At first, the (capacitive or magnetic) force will incrementally pull the movable electrode downward with increasing voltage. When the voltage

reaches a critical value, corresponding to an electrode displacement equal to 1/3 of the nominal (zero-voltage) gap, the movable electrode suddenly 'crashes' into the bottom electrode. In MEM relays, this problem is especially detrimental since they are necessarily operated within the pull-in region of the gap when the relay closes [19]. Obviously, repeated occurrence of pull-in will eventually damage the micro-relay. From a control perspective, the pull-in problem implies that MEM *relays* (as opposed to general MEM actuators) cannot be operated in an open loop manner. That is, *feedback* control is required for the relay to properly open and close without damage to the device.

Most MEM actuator feedback control work has been devoted to the electrostatic case. In [10, 11, 12], partial-state feedback control strategies were proposed using position and charge feedback along with a velocity observer. Control schemes based on differential flatness, control Lyapunov functions, backstepping, and input-to-state stabilization were reported in [20, 21]. A PD-type controller was developed in [3] for an electrostatically-actuated MEM optical switch. In [19], it was shown that voltage-controlled electrostatic and electromagnetic MEM relays have a common nonlinear dynamic structure. Using a generalized dynamic model, [19] constructed two nonlinear state feedback control schemes: a Lyapunov-based setpoint controller and a feedback linearization tracking controller.

In this paper, we introduce a new class of nonlinear feedbacks for voltage-driven electrostatic and electromagnetic MEM relays. We use Lyapunov theory to construct state feedback and partial-state feedback tracking controllers. In the latter, we only assume that the movable electrode position and the electrical state (i.e., charge or flux) are fed back since direct and/or precise measurements of electrode velocity are often not possible [11, 12, 20]. In this case, a model-based velocity observer is designed and incorporated into the feedback control. Lastly, we exploit input-to-state stability (ISS) theory [16, 17] to analyze the robustness of our state feedback controller to uncertainty in some of the system parameters. This makes it possible to quantify the effects of parameter uncertainty on the tracking error, in terms of an ISS overshoot.

The dynamic model of the MEM relay is presented in Section 2. The construction of the state feedback tracking controller is given in Section 3. The proof of the tracking result is presented in Section 4. Two extensions of our main result are presented in the following two sections. Section 5 discusses the observer design, while Section 6 presents the robustness analysis. A numerical simulation of the state feedback control is presented in Section 7. We close in Section 8 with a summary of our work.

2 System Model

Electrostatic and electromagnetic micro-relays share the nonlinear dynamic model [19]

$$\begin{aligned} m\ddot{x} + b\dot{x} + kx &= \alpha z^2 \\ \beta\dot{z} + \gamma(g_0 - x)z &= u, \end{aligned} \tag{1}$$

where

$$z = \begin{cases} q \\ \phi \end{cases} \qquad \alpha = \begin{cases} 1/(2\epsilon A) \\ 1/(2\mu A) \end{cases} \qquad \beta = \begin{cases} R \\ N \end{cases} \qquad \gamma = \begin{cases} 1/(\epsilon A) \\ R/(N\mu A), \end{cases} \tag{2}$$

the first (resp., second) row in (2) corresponds to the electrostatic (resp., electromagnetic) micro-relay, x is the position of the movable electrode such that $x = 0$ when it is in the open position, $m > 0$ is the movable electrode mass, $b > 0$ is the squeezed-film damping coefficient, $k > 0$ is the spring stiffness, $g_0 > 0$ denotes the gap when the movable electrode is in the open position, A is the movable electrode area, R is the resistance of the circuit, and $u = v$ with v being the input voltage. For the electrostatic micro-relay, q is the charge, and ϵ denotes the gap permittivity. For the electromagnetic micro-relay, ϕ denotes the flux, μ is the gap permeability, and N is the number of coil turns.

Remark 1. *Equation (1) models the micro-relay dynamics when there is no contact between the electrodes; i.e., $x \in (-\infty, g_0)$. When contact occurs, we assume that the kinetic energy of the movable electrode becomes zero so the dynamics is governed by $\beta \dot{z} = u$ and $x \equiv g_0$. That is, we assume that there is no bouncing of the movable electrode on the fixed electrode. For a dynamic model that includes contact bounce, see [13].*

3 Tracking Control Design

In what follows, all (in)equalities should be understood to hold globally unless otherwise indicated, and we omit the arguments of our functions when they are clear. By C^k, we will mean k times continuously differentiable. Consider a C^3 function $y_d : [0, \infty) \to \mathbb{R}$ that admits constants $m_1, m_2, m_3, m_4 > 0$ such that

$$\begin{aligned} &\text{(a)} \;\; m_1 \leq y_d(t) \leq m_2, \;\; |\dot{y}_d(t)| \leq m_3, \;\text{ and }\; |\ddot{y}_d(t)| \leq m_4 \;\; \forall t \geq 0, \;\text{ and} \\ &\text{(b)} \;\; m_4 + \kappa_2 m_3 < 0.9 \kappa_1 m_1 \end{aligned} \tag{3}$$

where $\kappa_1 = \frac{k}{m}$ and $\kappa_2 = \frac{b}{m}$. Our objective in this section is to design a feedback $u(x, \dot{x}, z, t)$ that forces the electrode position x to track the reference trajectory y_d. (See Section 5 for stability results for cases where only x and z can be measured, and Section 6 for situations where there is uncertainty regarding the values of the parameters of the model.) We require u to be continuous in t and C^1 in $(x, \dot{x}, z)$. Moreover, we wish to choose u so that it stabilizes x to y_d with arbitrarily fast local exponential convergence.

Remark 2. *The micro-relay control problem is usually set up as a regulation/setpoint problem; i.e., the command is a piecewise constant function that alternates the closing and opening of the relay. In this work, we will construct tracking controllers since it gives one the flexibility of selecting a reference trajectory that improves the micro-relay performance. For example, one can choose a smooth trajectory that minimizes both the velocity of the movable electrode as it approaches the fixed electrode during closing and overshoots during opening. Our conditions (3) on the reference trajectory are a consequence of the structure of (1) as we will show soon. In Section 7, we craft a reference trajectory that satisfies (3) while being physically compatible with a typical MEM relay operation.*

To make our control objective precise, consider the dynamics of $Y = (e_1, e_2, \zeta)$ where

$e_1 = x - y_d$, $e_2 = \dot{e}_1$,

$$\begin{aligned} \zeta(t) &= \sqrt{\tfrac{\alpha}{m}} z(t) - R_\mu(e_1(t), e_2(t), t), \\ R_\mu(e_1, e_2, t) &= \sqrt{\ddot{y}_d(t) + \kappa_2 \dot{y}_d(t) + \kappa_1 y_d(t) + \mu(e_1, e_2)}, \end{aligned} \tag{4}$$

and μ is a C^1 function that we will specify later that satisfies

$$|\mu(e_1, e_2)| \ \leq \ \frac{\kappa_1 m_1}{10} \tag{5}$$

everywhere. Note that (3) and (5) yield

$$0 \ < \ \underline{R} \ := \ \sqrt{0.9\kappa_1 m_1 - m_4 - \kappa_2 m_3} \ \leq \ R_\mu(e_1, e_2, t) \ \leq \ \sqrt{2\kappa_1 m_2} \ =: \ \overline{R}. \tag{6}$$

In particular, we allow $\mu \equiv 0$ in which case we write $R_0(t)$ instead of $R_\mu(e_1, e_2, t)$ since in that case it does not depend on the e_is. The change of feedback

$$u = \gamma\,(g_0 - x)\,z + \beta\sqrt{\frac{m}{\alpha}} v_1 \tag{7}$$

and elementary calculations give the $Y = (e_1, e_2, \zeta)$ dynamics

$$\left\{ \begin{array}{rcl} \dot{e}_1 &=& e_2 \\ \dot{e}_2 &=& -\kappa_1 e_1 - \kappa_2 e_2 + \mu(e_1, e_2) + \zeta^2 + 2\zeta R_\mu(e_1, e_2, t) \\ \dot{\zeta} &=& v_1 - \frac{1}{2R_\mu(e_1, e_2, t)} \left\{ \dddot{y}_d(t) + \kappa_2 \ddot{y}_d(t) + \kappa_1 \dot{y}_d(t) + \dot{\mu} \right\} \end{array} \right. \tag{8}$$

where $\dot{\mu}$ is the time derivative of μ along the trajectories of (8); i.e.,

$$\dot{\mu} \ = \ \frac{\partial \mu}{\partial e_1}(e_1, e_2) e_2 + \frac{\partial \mu}{\partial e_2}(e_1, e_2) \left[-\kappa_1 e_1 - \kappa_2 e_2 + \mu(e_1, e_2) + \zeta^2 + 2\zeta R_\mu(e_1, e_2, t) \right]. \tag{9}$$

We wish to show that for each constant $\mathcal{L} > 0$, we can find $\mu \in C^1$ satisfying (5) and a feedback $v_1 = v_1(e_1, e_2, \zeta, t)$ that is continuous in t and C^1 in (e_1, e_2, ζ) (with μ and v_1 depending on $\mathcal{L}$ in general) so that the following are true, in which $\underline{K}\mathcal{B}_3$ is the closed ball of radius $\underline{K}$ in $\mathbb{R}^3$ centered at the origin:

(S1) The system (8) in closed loop with v_1 is uniformly globally asymptotically stable (UGAS) to 0 [8].

(S2) There are constants $\underline{K}, \overline{K} > 0$ so that for all $t_o \geq 0$, and for all trajectories $Y(t)$ of (8) in closed loop with the feedback v_1 with initial values $Y(t_o) \in \underline{K}\mathcal{B}_3$, we have

$$|Y(t)| \ \leq \ \overline{K} e^{-\mathcal{L}(t - t_o)} |Y(t_o)| \quad \forall t \geq t_o \geq 0. \tag{10}$$

If these two objectives can be achieved for each constant $\mathcal{L} > 0$, then we say that (7) stabilizes x to y_d with arbitrarily fast local exponential convergence. For any given constant $a_2 > 0$ and $\overline{R}$ from (6), we also set

$$\Gamma = 16 \left[\sqrt{\frac{2}{\kappa_1}} + K \right]^2 \left(1 + \overline{R}^2 \right) + 1, \ \text{ where } \ K = \max \left\{ 2, \frac{2}{\kappa_1}, \frac{2}{\kappa_2} + \frac{(\kappa_2 + a_2)^2}{\kappa_1 \kappa_2} \right\}. \tag{11}$$

The following theorem shows how our stabilization objectives can indeed be realized:

Theorem 1. *Let a_1 and a_2 be any given positive constants and set $\sigma(s) = s/\sqrt{1+s^2}$ and*

$$\mu(e_1, e_2) = -\frac{\kappa_1 m_1}{20}\left[\sigma\left(\frac{20a_1}{\kappa_1 m_1}e_1\right) + \sigma\left(\frac{20a_2}{\kappa_1 m_1}e_2\right)\right]. \tag{12}$$

Then for any constant a_3 for which

$$a_3 \;\geq\; \frac{4}{\underline{R}}\left\{1 + \Gamma\left(\frac{1}{\kappa_1}+1\right)\right\}\{a_1 + a_2(1 + 2\overline{R} + \kappa_1 + \kappa_2 + a_1 + a_2)\}, \tag{13}$$

the feedback

$$v_1(e_1, e_2, \zeta, t) \;=\; -a_3\zeta(1+\zeta^2) + \frac{1}{2R_\mu(e_1, e_2, t)}\{\dddot{y}_d(t) + \kappa_2\ddot{y}_d(t) + \kappa_1\dot{y}_d(t)\} \tag{14}$$

renders (8) UGAS to the origin. Moreover, for each constant $\mathcal{L} > 0$, we can choose values of the constants a_i and $\underline{K}, \overline{K} > 0$ so that all trajectories of (8) in closed loop with (14) that start in $\underline{K}\mathcal{B}_3$ satisfy (10). Hence, (7) with the choice (14) stabilizes x to y_d with arbitrarily fast local exponential convergence.

Remark 3. *An important byproduct of our proof of Theorem 1 will be the explicit construction of a strict Lyapunov function for the closed loop dynamics (8), namely,*

$$\begin{aligned}
&V_3(e_1, e_2, \zeta) = V_2(e_1, e_2) + \Gamma Q(\zeta), \quad \textit{where}\\
&V_2(e_1, e_2) = e_1 e_2 + KV_1(e_1, e_2), \;\; Q(\zeta) = \tfrac{1}{a_3}\left(\tfrac{1}{2}\zeta^2 + \tfrac{1}{4}\zeta^4\right),\\
&V_1(e_1, e_2) = \tfrac{1}{2}e_2^2 + \int_0^{e_1}\left\{\kappa_1 l + \frac{\kappa_1 m_1}{20}\sigma\left(\frac{20a_1}{\kappa_1 m_1}l\right)\right\}dl,
\end{aligned} \tag{15}$$

Γ and K are defined in (11), and the constants $a_i > 0$ will be chosen later. One advantage of having Lyapunov functions is that they can often be used to quantify the effects of uncertainty in the parameters in the model. For example, our Lyapunov approach can be used to give tracking that is robust to small uncertainties on the parameters k and b from (1), in the sense of input-to-state stability; see Section 6 below.

Remark 4. *Theorem 1 remains true (with the same proof) if we replace $\sigma(s) = s/\sqrt{1+s^2}$ with any C^2 function $\sigma : \mathbb{R} \to [-1, +1]$ for which (I) $\sigma(0) = 0$, $\sigma'(0) = 1$, and $0 \leq \sigma' \leq 1$ everywhere and (II) $s \mapsto s\sigma(s)$ is positive definite. We made our particular choice of σ to simplify the statement of the theorem.*

Remark 5. *The simpler feedback $v_1 = -\zeta + \{\dddot{y}_d(t) + \kappa_2\ddot{y}_d(t) + \kappa_1\dot{y}_d(t)\}/\{2R_0(t)\}$ and the choice $\mu \equiv 0$ also render (8) UGAS to 0. To see why, note that the time derivative of the proper positive definite function*

$$\begin{aligned}
&V_o(e_1, e_2, \zeta) = Ae_1^2 + e_2^2 + Be_1e_2 + C(\zeta^2 + \zeta^4), \quad \textit{where}\\
&A = \kappa_1 + \tfrac{B\kappa_2}{2}, \;\; B = \min\left\{\kappa_2, \sqrt{\kappa_1}\right\}, \;\; \textit{and} \;\; C = \max\left\{\tfrac{1}{\kappa_2} + \tfrac{B}{4\kappa_1}, \tfrac{1}{4} + \tfrac{16\kappa_1 m_2}{\kappa_2} + 4Bm_2\right\}
\end{aligned}$$

along the trajectories of $[\dot{e}_1 = e_2,\ \dot{e}_2 = -\kappa_1 e_1 - \kappa_2 e_2 + \zeta^2 + 2\zeta R_0,\ \dot{\zeta} = -\zeta]$ *satisfies*

$$\begin{aligned}
\dot{V}_o &= -B\kappa_1 e_1^2 + (B - 2\kappa_2)e_2^2 + (2e_2 + Be_1)[\zeta^2 + 2\zeta R_0] - C(2\zeta^2 + 4\zeta^4) \\
&\leq -B\kappa_1 e_1^2 - \kappa_2 e_2^2 + \{\sqrt{\kappa_2} e_2\} \left\{ \tfrac{2}{\sqrt{\kappa_2}} \left(\zeta^2 + 2\zeta R_0\right) \right\} + B\{\sqrt{\kappa_1} e_1\} \left\{ \tfrac{1}{\sqrt{\kappa_1}} (\zeta^2 + 2\zeta R_0) \right\} \\
&\quad -C(2\zeta^2 + 4\zeta^4) \\
&\leq -\tfrac{B\kappa_1}{2} e_1^2 - \tfrac{\kappa_2}{2} e_2^2 + \left[\tfrac{4}{\kappa_2} + \tfrac{B}{\kappa_1} \right] (\zeta^4 + 4\zeta^2 R_0^2) - C(2\zeta^2 + 4\zeta^4) \\
&\leq -\tfrac{B\kappa_1}{2} e_1^2 - \tfrac{\kappa_2}{2} e_2^2 - \tfrac{1}{2}\zeta^2,
\end{aligned}$$

where we applied the relation $pq \leq p^2/2 + q^2/2$ *to the terms in braces and (6). However, this simpler feedback would not guarantee arbitrarily fast local exponential convergence. See Section 4.2 for the proof that (14) leads to arbitrarily fast local exponential convergence, and a discussion of the importance of this result.*

4 Proof of Theorem 1

4.1 Proof of UGAS of Closed-Loop System

We show that (8) in closed loop with (14) admits the Lyapunov function (15) when the a_is satisfy (13). First consider the reduced (e_1, e_2)-subdynamics of (8) with μ defined in (12) and ζ equal to zero; i.e.,

$$\left\{ \begin{array}{rcl} \dot{e}_1 &=& e_2 \\ \dot{e}_2 &=& -\kappa_1 e_1 - \frac{\kappa_1 m_1}{20} \sigma \left(\frac{20 a_1}{\kappa_1 m_1} e_1 \right) - \kappa_2 e_2 - \frac{\kappa_1 m_1}{20} \sigma \left(\frac{20 a_2}{\kappa_1 m_1} e_2 \right). \end{array} \right. \tag{16}$$

The function V_1 in (15) has the time derivative $\dot{V}_1 \leq -\kappa_2 e_2^2$ along the trajectories of (16). By properties (I)-(II) from Remark 4, the time derivative of $T(e_1, e_2) = e_1 e_2$ along the trajectories of (16) satisfies

$$\begin{aligned}
\dot{T} &= e_2^2 - \kappa_1 e_1^2 - \tfrac{\kappa_1 m_1}{20} e_1 \sigma \left(\tfrac{20 a_1}{\kappa_1 m_1} e_1 \right) - \kappa_2 e_1 e_2 - \tfrac{\kappa_1 m_1}{20} e_1 \sigma \left(\tfrac{20 a_2}{\kappa_1 m_1} e_2 \right) \\
&\leq e_2^2 - \kappa_1 e_1^2 + \left\{ \tfrac{(\kappa_2 + a_2)|e_2|}{\sqrt{\kappa_1}} \right\} \left\{ \sqrt{\kappa_1} |e_1| \right\} \\
&\leq \left(1 + \tfrac{(\kappa_2 + a_2)^2}{2\kappa_1} \right) e_2^2 - \tfrac{1}{2} \kappa_1 e_1^2,
\end{aligned} \tag{17}$$

by applying the general relation $pq \leq p^2/2 + q^2/2$ to the terms in braces. Hence, along the trajectories of (16), the time derivative of V_2 from (15) satisfies $\dot{V}_2 \leq -W_2(e_1, e_2)$, where $W_2(e_1, e_2) = e_2^2 + \kappa_1 e_1^2/2$. Moreover, $V_2(e_1, e_2) \geq K e_2^2/4 + K\kappa_1 e_1^2/4$ everywhere.

Since $\frac{\partial V_2}{\partial e_2}(e_1, e_2) = e_1 + K e_2$, the time derivative of V_2 along the solutions of the full system (8) satisfies

$$\begin{aligned}
\dot{V}_2 &\leq -W_2(e_1, e_2) + \tfrac{\partial V_2}{\partial e_2}(e_1, e_2) \left[\zeta^2 + 2\zeta R_\mu(e_1, e_2, t) \right] \\
&\leq -W_2(e_1, e_2) + \sqrt{W_2(e_1, e_2)} \left\{ \left[\tfrac{\sqrt{2}}{\sqrt{\kappa_1}} + K \right] \left[\zeta^2 + 2\overline{R}|\zeta| \right] \right\} \\
&\leq -\tfrac{1}{2} W_2(e_1, e_2) + \left[\tfrac{\sqrt{2}}{\sqrt{\kappa_1}} + K \right]^2 (\zeta^4 + 4\overline{R}^2 \zeta^2),
\end{aligned} \tag{18}$$

where we again applied the general relation $pq \leq \frac{1}{2}p^2 + \frac{1}{2}q^2$. Recalling (9) and the fact that $|\sigma'| \leq 1$ everywhere, we get

$$\frac{1}{2\underline{R}}|\dot{\mu}| \ \leq \ \overline{L}(|e_1|+|e_2|+|\zeta|+\zeta^2), \ \text{ where } \ \overline{L} := \frac{1}{2\underline{R}}\{a_1+a_2(1+2\overline{R}+\kappa_1+\kappa_2+a_1+a_2)\}. \quad (19)$$

Hence, the time derivative of Q from (15) along the closed loop trajectories of (8) satisfies

$$\begin{aligned}
\dot{Q} &\leq -[\zeta^2+\zeta^4+\zeta^6] + \tfrac{1}{2\underline{R}a_3}(|\zeta|+|\zeta|^3)|\dot{\mu}| \\
&\leq -[\zeta^2+\zeta^4+\zeta^6] + \tfrac{\overline{L}}{a_3}(|\zeta|+|\zeta|^3)(|e_1|+|e_2|+|\zeta|+\zeta^2) \\
&\leq -[\zeta^2+\zeta^4+\zeta^6] + \tfrac{\overline{L}}{a_3}(e_1^2+e_2^2+2\zeta^2+|\zeta|^3+\zeta^4+|\zeta|^5+\zeta^6) \qquad (20) \\
&\leq -\left(1-\tfrac{6\overline{L}}{a_3}\right)[\zeta^2+\zeta^4+\zeta^6] + \tfrac{\overline{L}}{a_3}(e_1^2+e_2^2) \\
&\leq -\tfrac{1}{4}[\zeta^2+\zeta^4] + \tfrac{1}{8\Gamma}\kappa_1 e_1^2 + \tfrac{1}{4\Gamma}e_2^2
\end{aligned}$$

by separately considering the cases $|\zeta| \geq 1$ and $|\zeta| < 1$, and then using the general relation $pq \leq \frac{1}{2}p^2+\frac{1}{2}q^2$ and the fact that a_3 satisfies (13). Hence, our proper positive definite function V_3 from (15) satisfies

$$\dot{V}_3 \ \leq \ -\{W_2(e_1,e_2)+\zeta^2+\zeta^4\}/4$$

and so is a Lyapunov function for the dynamics, proving the UGAS assertion of the theorem.

4.2 Proof of Arbitrarily Fast Local Exponential Convergence

The structure of the system dynamics (viz., the term z^2 in (1)) is responsible for the constraint (5) on the feedback, and thereby on the closed-loop system performance. In particular, this constraint restricts the *global* rate of convergence of the tracking error. Therefore, it is desirable that the control, at least, yield arbitrarily fast *local* convergence. We prove that this objective is achieved with the proposed feedback.

We first linearize (8) around 0 in closed loop with our feedback v_1 to get

$$\left\{\begin{array}{rcl}
\dot{e}_{1l} &=& e_{2l} \\
\dot{e}_{2l} &=& -(\kappa_1+a_1)e_{1l} - (\kappa_2+a_2)e_{2l} + 2\zeta_l R_0(t) \\
\dot{\zeta}_l &=& -\tfrac{a_2}{2R_0}[a_1+\kappa_1]e_{1l} - \tfrac{1}{2R_0}(\kappa_2 a_2 - a_1 + a_2^2)e_{2l} - (a_3-a_2)\zeta_l.
\end{array}\right. \qquad (21)$$

Set $e_l = (e_{1l}, e_{2l})$. Choose $a_1 = -\kappa_1 + \eta^2$ and $a_2 = -\kappa_2 + 2\eta$, with η sufficiently large so that a_1 and a_2 are positive. Consider the function $Q_a(e_l) = (\eta+\eta^{3/2})e_{1l}^2 + e_{2l}^2/\sqrt{\eta} + e_{1l}e_{2l}$. When $\eta > 0$ is sufficiently large, we have $|e_l|^2/(2\sqrt{\eta}) \leq Q_a(e_l) \leq 3\eta^{3/2}e_{1l}^2 + 2e_{2l}^2$ everywhere. Hence, along all trajectories of (21), we get

$$\dot{Q}_a \ = \ -\eta^2 e_{1l}^2 + (1-4\sqrt{\eta})e_{2l}^2 + 2\frac{\partial Q_a}{\partial e_{2l}}(e_l)\zeta_l R_o(t) \ \leq \ -\frac{1}{3}\sqrt{\eta}Q_a(e_l) + 4||e_l||\zeta_l|\bar{R}$$

for sufficiently large η. Therefore, the time derivative of $Q_b(e_{1l}, e_{2l}, \zeta_l) := Q_a(e_l) + \frac{1}{2}\zeta_l^2$ satisfies

$$\begin{aligned}
\dot{Q}_b &\leq -\tfrac{1}{3}\sqrt{\eta}Q_a(e_l) + 4\overline{R}|\zeta_l||e_l| - (a_3-a_2)\zeta_l^2 \\
&\quad + \tfrac{1}{2R_0}|\zeta_l|\left[a_2(a_1+\kappa_1)|e_{1l}| + (\kappa_2 a_2 + a_1 + a_2^2)|e_{2l}|\right] \\
&\leq -\tfrac{1}{3}\sqrt{\eta}Q_a(e_l) - (a_3-a_2)\zeta_l^2 + \{2K'|\zeta_l|\}\tfrac{|e_l|}{2}, \\
&\quad \text{where } K' = 4\overline{R} + \tfrac{1}{\underline{R}}\{a_2(a_1+\kappa_1) + \kappa_2 a_2 + a_1 + a_2^2\}
\end{aligned}$$

along the trajectories of (21). Applying the relation $pq \leq p^2/2 + q^2/2$ with $p = 2K'|\zeta_l|$ and $q = |e_l|/2$ and enlarging a_3 and η as necessary, we can ensure that $\dot{Q}_b \leq -\frac{1}{12}\sqrt{\eta}Q_b$ along the trajectories of (21). Moreover, $|(e_l, \zeta_l)|^2/(2\sqrt{\eta}) \leq Q_b(e_l, \zeta_l) \leq 3\eta^{3/2}|(e_l, \zeta_l)|^2$ everywhere when $\eta > 0$ is large enough. The arbitrarily fast exponential stability assertion from the theorem now follows from a standard linearization principle.

5 Observer Design

The controller from Theorem 1 requires precise measurements of $\dot{x}$ which may not be available in practice [11, 12, 20]. On the other hand, our methods can be adapted to design an observer that regulates the errors e_1 and e_2 to zero, even if only x and z are available for measurement. To see why, consider the observer

$$\left\{\begin{array}{rcl} \dot{\hat{e}}_1 &=& \hat{e}_2 + L_1(e_1 - \hat{e}_1) \\ \dot{\hat{e}}_2 &=& -\kappa_1 e_1 - \kappa_2 \hat{e}_2 - \ddot{y}_d(t) - \kappa_2 \dot{y}_d(t) - \kappa_1 y_d(t) + \frac{\alpha}{m} z^2 + L_2(e_1 - \hat{e}_1), \end{array}\right. \tag{22}$$

where the L_is are any positive constants for which $L_2 > 2L_1(L_1 + 8\kappa_2)$. The system (22) depends only on x, z, and y_d. We continue to assume that y_d admits constants $m_1, \ldots, m_4 > 0$ satisfying (3). Defining $\tilde{e}_i = e_i - \hat{e}_i$ for $i = 1$ and 2, defining μ and v_1 as in (12) and (14), and taking

$$v_1 := v_1(\hat{e}_1, \hat{e}_2, \hat{\zeta}, t) \text{ and } \mu := \mu(\hat{e}_1, \hat{e}_2)$$

in (8) (for any constants $a_i > 0$ satisfying the hypotheses of Theorem 1) easily yields the system

$$\left\{\begin{array}{rcl} \dot{\hat{e}}_1 &=& \hat{e}_2 + L_1\tilde{e}_1 \\ \dot{\hat{e}}_2 &=& -\kappa_1\hat{e}_1 - \kappa_2\hat{e}_2 + \mu(\hat{e}_1, \hat{e}_2) + \hat{\zeta}^2 + 2\hat{\zeta}R_\mu(\hat{e}_1, \hat{e}_2, t) + (L_2 - \kappa_1)\tilde{e}_1 \\ \dot{\hat{\zeta}} &=& v_1(\hat{e}_1, \hat{e}_2, \hat{\zeta}, t) - \frac{1}{2R_\mu(\hat{e}_1, \hat{e}_2, t)}\left\{\dddot{y}_d(t) + \kappa_2\ddot{y}_d + \kappa_1\dot{y}_d + \dot{\mu}\right\} \\ \dot{\tilde{e}}_1 &=& \tilde{e}_2 - L_1\tilde{e}_1 \\ \dot{\tilde{e}}_2 &=& -\kappa_2\tilde{e}_2 - L_2\tilde{e}_1, \end{array}\right. \tag{23}$$

where $\hat{\zeta} = \sqrt{\frac{\alpha}{m}}z(t) - R_\mu(\hat{e}_1, \hat{e}_2, t)$, R_μ is as defined in (4), and

$$\begin{array}{rcl} \dot{\mu} &=& \frac{\partial\mu}{\partial\hat{e}_1}(\hat{e}_1, \hat{e}_2)(\hat{e}_2 + L_1\tilde{e}_1) \\ && + \frac{\partial\mu}{\partial\hat{e}_2}(\hat{e}_1, \hat{e}_2)\left[-\kappa_1\hat{e}_1 - \kappa_2\hat{e}_2 + \mu(\hat{e}_1, \hat{e}_2) + \hat{\zeta}^2 + 2\hat{\zeta}R_\mu(\hat{e}_1, \hat{e}_2, t) + (L_2 - \kappa_1)\tilde{e}_1\right]. \end{array} \tag{24}$$

Set $\hat{e} = (\hat{e}_1, \hat{e}_2)$. The fact that e_1 and e_2 are regulated to zero follows immediately from:

Theorem 2. *The system (23) is UGAS to the origin. Moreover, by choosing the L_is and a_is to be appropriate constants, we can ensure that (23) is UGAS to 0 with arbitrarily fast local exponential convergence.*

Proof. Set $\tilde{V}_3(\hat{e}_1, \hat{e}_2, \hat{\zeta}) = V_2(\hat{e}_1, \hat{e}_2) + \Gamma Q(\hat{\zeta})$ where V_2 and Q are from (15) and Γ is from (11). By the argument of Section 4.1, the time derivative of $\tilde{V}_3$ along the trajectories of (23) satisfies

$$\begin{array}{rcl} \dot{\tilde{V}}_3 &\leq& -\frac{1}{4}W_2(\hat{e}_1, \hat{e}_2) - \frac{1}{4}[\hat{\zeta}^2 + \hat{\zeta}^4] + \frac{\partial\tilde{V}_2}{\partial\hat{e}_1}(\hat{e}_1, \hat{e}_2)L_1\tilde{e}_1 + \frac{\partial\tilde{V}_2}{\partial\hat{e}_2}(\hat{e}_1, \hat{e}_2)(L_2 - \kappa_1)\tilde{e}_1 \\ && + \Gamma\frac{\partial Q}{\partial\hat{\zeta}}(\hat{\zeta})\left[-\frac{1}{2R_\mu(\hat{e}_1, \hat{e}_2, t)}\right]\left[\frac{\partial\mu}{\partial\hat{e}_1}(\hat{e}_1, \hat{e}_2)L_1\tilde{e}_1 + \frac{\partial\mu}{\partial\hat{e}_2}(\hat{e}_1, \hat{e}_2)(L_2 - \kappa_1)\tilde{e}_1\right]. \end{array} \tag{25}$$

By elementary calculations, one can determine a constant $\Omega_1 > 0$ such that

$$\begin{aligned}\dot{\tilde{V}}_3 &\leq -\Omega_2(\hat{e}_1^2+\hat{e}_2^2) - \tfrac{1}{4}[\hat{\zeta}^2+\hat{\zeta}^4] + \left\{\Omega_1|\tilde{e}_1|/\sqrt{\Omega_2}\right\}\left\{|\hat{e}|\sqrt{\Omega_2}\right\} + \Omega_1|\hat{\zeta}+\hat{\zeta}^3||\tilde{e}_1| \\ &\leq -\tfrac{1}{2}\Omega_2(\hat{e}_1^2+\hat{e}_2^2) - \tfrac{1}{4}[\hat{\zeta}^2+\hat{\zeta}^4] + (\Omega_1^2/\Omega_2)\tilde{e}_1^2 + \Omega_1|\hat{\zeta}+\hat{\zeta}^3||\tilde{e}_1| \\ &\leq -\tfrac{1}{2}\Omega_2(\hat{e}_1^2+\hat{e}_2^2) - \tfrac{1}{8}[\hat{\zeta}^2+\hat{\zeta}^4] + [(\Omega_1^2/\Omega_2)+2\Omega_1^2]\,\tilde{e}_1^2 + 8^3\Omega_1^4\tilde{e}_1^4,\end{aligned} \tag{26}$$

where $\Omega_2 = \min\{1, \kappa_1/2\}/4$ and we used the relations $pq \leq p^2/2 + q^2/2$ for $p, q \geq 0$,

$$\Omega_1|\hat{\zeta}||\tilde{e}_1| \;\leq\; 2\Omega_1^2\tilde{e}_1^2 + \frac{1}{8}\hat{\zeta}^2, \;\text{ and }\; \{8^{3/4}\Omega_1|\tilde{e}_1|\}\{8^{-3/4}|\hat{\zeta}|^3\} \;\leq\; 8^3\Omega_1^4\tilde{e}_1^4 + \frac{1}{8}\tilde{\zeta}^4$$

where the last inequality is a special case of Hölder's Inequality.

By our assumption that $L_2 > 2L_1(L_1 + 8\kappa_2)$, the function

$$M(\tilde{e}_1, \tilde{e}_2) = \tfrac{L_2}{2}\tilde{e}_1^2 + \tfrac{1}{2}\tilde{e}_2^2 - \tfrac{L_1}{2}\tilde{e}_1\tilde{e}_2$$

is proper and positive definite. Moreover, using the relation $pq \leq \frac{1}{2\delta}p^2 + \frac{\delta}{2}q^2$ with $p = 0.5L_1\tilde{e}_1$, $q = (L_1+\kappa_2)\tilde{e}_2$, and $\delta = L_1/(2L_2)$, one checks that M has the time derivative

$$\begin{aligned}\dot{M} &= -\tfrac{L_1L_2}{2}\tilde{e}_1^2 - \left(\tfrac{L_1}{2}+\kappa_2\right)\tilde{e}_2^2 + \{0.5L_1\tilde{e}_1\}\{(L_1+\kappa_2)\tilde{e}_2\} \\ &\leq -\tfrac{L_1L_2}{4}\tilde{e}_1^2 - \left(\tfrac{L_1}{2}+\kappa_2 - \tfrac{L_1}{4L_2}(L_1+\kappa_2)^2\right)\tilde{e}_2^2 \\ &= L_1\left[-\tfrac{L_2}{4}\tilde{e}_1^2 - \left(\tfrac{1}{2}+\tfrac{\kappa_2}{L_1} - \tfrac{1}{4L_2}(L_1+\kappa_2)^2\right)\tilde{e}_2^2\right]\end{aligned}$$

along the trajectories of the $(\tilde{e}_1, \tilde{e}_2)$-subsystem of (23). Since $L_2 > L_1^2$, we get

$$-\frac{L_2}{8}\tilde{e}_1^2 - \frac{1}{4}\tilde{e}_2^2 \;\leq\; \frac{L_1}{8}\tilde{e}_1\tilde{e}_2,$$

by the relation $pq \geq -p^2 - \frac{1}{4}q^2$ with $p = L_1\tilde{e}_1/8$ and $q = \tilde{e}_2$. Since $L_2 > 2L_1(L_1+8\kappa_2)$, it follows that

$$\begin{aligned}\dot{M} &\leq L_1\left[-\tfrac{L_2}{8}\tilde{e}_1^2 - \left(\tfrac{1}{4}+\tfrac{\kappa_2}{L_1} - \tfrac{1}{4L_2}(L_1+\kappa_2)^2\right)\tilde{e}_2^2 + \tfrac{L_1}{8}\tilde{e}_1\tilde{e}_2\right] \\ &\leq -\tfrac{L_1}{4}M - L_1\left(\tfrac{1}{8}+\tfrac{\kappa_2}{L_1} - \tfrac{1}{4L_2}(L_1+\kappa_2)^2\right)\tilde{e}_2^2 \;\leq\; -\tfrac{L_1}{4}M.\end{aligned} \tag{27}$$

Since L_1 can be freely chosen, it follows from the last inequality that one can obtain an arbitrarily large rate of convergence for the variables $\tilde{e}_1$ and $\tilde{e}_2$ by choosing L_1 sufficiently large.

Moreover, elementary calculations provide a constant $\Omega_4 > 0$ such that the time derivative of

$$V_4 \;=\; \tilde{V}_3(\hat{e}_1, \hat{e}_2, \hat{\zeta}) + \Omega_4[M(\tilde{e}_1, \tilde{e}_2) + M(\tilde{e}_1, \tilde{e}_2)^2]$$

along the trajectories of (23) satisfies $\dot{V}_4 \leq -\frac{1}{2}\Omega_2(\hat{e}_1^2+\hat{e}_2^2) - \frac{1}{8}[\hat{\zeta}^2+\hat{\zeta}^4] - \tilde{e}_1^2 - \tilde{e}_2^2$. Since V_4 is positive definite and radially unbounded, it is a strict Lyapunov function for the system (23), which gives the UGAS of (23). Combining (27) with the arguments from Section 4.2 (using the Lyapunov function $Q_b + M$ for the linearization of (23) where Q_b is from Section 4.2), we deduce that one can obtain arbitrarily fast local exponential convergence for (23) using appropriate choices of the constants a_i and L_i. ∎

6 Robustness Analysis

Suppose now that the parameter k in (1) is not known with certainty. This situation can be modeled by replacing k in (1) with $k + \varepsilon m$, where k represents a nominal (or estimated) value of the parameter, m is the electrode mass as before, and ε represents uncertainty. We specify our admissible values of ε shortly. Our objective in this section is to quantify the effects of ε on the performance of our feedbacks (see Remark 7 below for the analogous case where there is uncertainty in the parameter b). For simplicity, we assume that ε is constant but the general case where ε is time dependent can be handled by analogous arguments. Replacing k with $k + \varepsilon m$ in the original model (1), changing variables as before, and taking the feedback

$$v_1 = -\lambda^6\zeta(1+\zeta^2) + \frac{1}{2R_\mu(e_1,e_2,t)}\left\{\dddot{y}_d(t) + \kappa_2\ddot{y}_d(t) + \kappa_1\dot{y}_d(t)\right\} \tag{28}$$

where $\lambda > 0$ is a constant we will specify below gives the $Y = (e_1, e_2, \zeta)$ dynamics

$$\left\{\begin{array}{rcl} \dot{e}_1 &=& e_2 \\ \dot{e}_2 &=& -\kappa_1 e_1 - \kappa_2 e_2 + \mu(e_1,e_2) + \zeta^2 + 2\zeta R_\mu(e_1,e_2,t) - \varepsilon(e_1 + y_d) \\ \dot{\zeta} &=& -\lambda^6\zeta(1+\zeta^2) - \frac{\dot{\mu}}{2R_\mu(e_1,e_2,t)} \end{array}\right. \tag{29}$$

where μ is a function we choose later that will satisfy $|\mu(e_1,e_2)| \leq \frac{1}{2}\kappa_1 m_1$ everywhere and $\dot{\mu}$ is now calculated along the e-subdynamics of (29). We wish to show that μ can be chosen so that (29) is *input-to-state stable (ISS) with respect to ε with arbitrarily small linear overflows.* The relevant definitions are as follows.

We say that (29) (with prescribed choices of λ and μ) is ISS with respect to ε provided there exist functions $\beta \in \mathcal{KL}$ and $\Delta \in \mathcal{K}_\infty$ so that all trajectories $Y(t)$ of (29) for all initial values $Y(t_o)$ satisfy $|Y(t)| \leq \beta(|Y(t_o)|, t - t_o) + \Delta(|\varepsilon|)$ for all $t \geq t_o \geq 0$.[1] If Δ has the form $\Delta(r) = \overline{\gamma}r$ for some constant $\overline{\gamma} > 0$, then we call $\overline{\gamma}$ the *overflow rate*. The ISS condition reduces to the standard UGAS condition when the uncertainty ε is zero, but it is far more general because it quantifies the effects of ε in terms of the overshoot term $\Delta(|\varepsilon|)$. In particular, ISS of (29) implies that the tracking error $|e_1(t)| = |x(t) - y_d(t)| \to 0$ as $t \to +\infty$ with an overshoot that can be quantified to be small when ε is suitably small. We say that (29) can be made ISS with respect to ε *with arbitrarily small linear overflows* provided we can find $\beta \in \mathcal{KL}$ satisfying: For each constant $\overline{\gamma} > 0$, we can choose our function μ and a positive constant λ (both depending on $\overline{\gamma}$) so that all trajectories $Y(t)$ of (29) for all initial values $Y(t_o)$ satisfy $|Y(t)| \leq \beta(|Y(t_o)|, t - t_o) + \overline{\gamma}|\varepsilon|$ for all $t \geq t_o \geq 0$. In other words, we can choose the feedback to make the overflow rate $\overline{\gamma}$ as small as desired.

To prove our ISS properties, we use the Lyapunov function from Remark 5 except with ζ set to zero; i.e.,

$$\tilde{V}_o(e_1,e_2) = Ae_1^2 + e_2^2 + Be_1e_2, \text{ where } A = \kappa_1 + \frac{B\kappa_2}{2} \text{ and } B = \min\left\{\kappa_2, \sqrt{\kappa_1}\right\}. \tag{30}$$

[1] A function $\delta : [0,\infty) \to [0,\infty)$ is *positive definite* provided $\delta(0) = 0$ and $\delta(r) > 0$ for all $r > 0$. A positive definite function δ is *of class* $\mathcal{K}_\infty$ (written $\delta \in \mathcal{K}_\infty$) provided it is strictly increasing and unbounded. A continuous function $\beta : [0,\infty) \times [0,\infty) \to [0,\infty)$ is *of class* $\mathcal{KL}$ (written $\beta \in \mathcal{KL}$) provided (a) $\beta(\cdot, t) \in \mathcal{K}_\infty$ for each $t \geq 0$, (b) $\beta(s,\cdot)$ is nonincreasing for each $s \geq 0$, and (c) for each $s \geq 0$, $\beta(s,t) \to 0$ as $t \to +\infty$.

By separately considering the cases $B = \kappa_2$ and $B = \sqrt{\kappa_1}$, we easily check the global inequalities

$$\begin{array}{l} \omega_1(e_1^2+e_2^2) \;\le\; \tilde{V}_o(e_1,e_2) \;\le\; \omega_2(e_1^2+e_2^2), \\ \text{where } \omega_1 = \frac{1}{2}\min\{\kappa_1,1\} \text{ and } \omega_2 = \max\{A,1\} + \frac{B}{2}. \end{array} \tag{31}$$

To stipulate the necessary values of λ and ε, we also use the constants

$$\begin{array}{l} \theta = \frac{c\omega_1}{20(4+B^2)}, \;\; c = \frac{\min\{B\kappa_1,\kappa_2\}}{B+2\max\{A,1\}}, \;\; M = \frac{1}{\theta}\max\left\{1, 4\overline{R}^2\right\}, \\ \text{and } \tilde{\mathcal{L}} = \kappa_1 m_1\left\{2(\kappa_1[m_1+1]+\kappa_2+2\overline{R}) + 3B\kappa_1 m_2 + 2m_2 + 2 + B\right\}, \end{array} \tag{32}$$

where $\overline{R}$ is defined in (6) and the m_is are from (3). We first assume that the uncertainty ε satisfies

$$|\varepsilon| \le \min\left\{\tfrac{9B\kappa_1}{20(B+1)}, \tfrac{9\kappa_2}{20}, \tfrac{2\kappa_1 m_1}{5m_2}\right\} \tag{33}$$

but see Remark 6 for ISS results under less stringent bounds on ε, and see Section 7 where our bounds are computed explicitly. Our main robustness result is as follows:

Theorem 3. *For each constant $\lambda > 2 + \frac{9\tilde{\mathcal{L}}}{\underline{R}}(\frac{1}{\sqrt{c\omega_1}}+1)(M+1)$, the choice*

$$\mu(e_1,e_2) = -\frac{9}{20}\kappa_1 m_1 \sigma\left(\lambda\frac{\partial\tilde{V}_o}{\partial e_2}(e_1,e_2)\right) \tag{34}$$

with $\sigma(s) = s/\sqrt{1+s^2}$ renders (29) ISS with respect to uncertainties ε satisfying (33). In fact, by choosing μ as in (34) and λ appropriately, we can make (29) ISS with respect to ε with arbitrarily small linear overflows.

Proof. Arguing as in Remark 5, one easily shows that the time derivative of $\tilde{V}_o$ along the trajectories of

$$\left\{\begin{array}{rcl} \dot{e}_1 &=& e_2 \\ \dot{e}_2 &=& -\kappa_1 e_1 - \kappa_2 e_2 + \mu(e_1,e_2) - \varepsilon(e_1+y_d) \end{array}\right. \tag{35}$$

satisfies

$$\dot{\tilde{V}}_0 \le -\frac{B\kappa_1}{2}e_1^2 - \frac{\kappa_2}{2}e_2^2 + \frac{\partial\tilde{V}_0}{\partial e_2}(e_1,e_2)\left[\mu(e_1,e_2) - \varepsilon(e_1+y_d)\right]. \tag{36}$$

From our condition (33) on ε, it follows that

$$\left|\frac{\partial\tilde{V}_0}{\partial e_2}(e_1,e_2)\varepsilon e_1\right| \;\le\; \left[(B+1)e_1^2+e_2^2\right]|\varepsilon| \;\le\; \frac{9B\kappa_1}{20}e_1^2 + \frac{9\kappa_2}{20}e_2^2. \tag{37}$$

Combining (36) and (37), it follows that the time derivative of $\tilde{V}_o$ along the trajectories of (35) satisfies

$$\begin{array}{rcl} \dot{\tilde{V}}_o &\le& -\frac{c}{10}\tilde{V}_o + \frac{\partial\tilde{V}_o}{\partial e_2}(e_1,e_2)\left[-\frac{9}{20}\kappa_1 m_1\sigma\left(\lambda\frac{\partial\tilde{V}_o}{\partial e_2}(e_1,e_2)\right) - \varepsilon y_d\right] \\ &\le& -\frac{c}{10}\tilde{V}_o - \frac{9}{20}\kappa_1 m_1\left|\frac{\partial\tilde{V}_o}{\partial e_2}(e_1,e_2)\right|\sigma\left(\lambda\left|\frac{\partial\tilde{V}_o}{\partial e_2}(e_1,e_2)\right|\right) + |\varepsilon y_d|\left|\frac{\partial\tilde{V}_o}{\partial e_2}(e_1,e_2)\right|, \end{array} \tag{38}$$

by our choices of c and σ and (31). Consider two cases:

1) $\lambda \left|\frac{\partial \tilde{V}_o}{\partial e_2}(e_1,e_2)\right| \geq \frac{9}{4}$. Then, since $|\sigma(r)| \geq \frac{9}{10}$ for $|r| \geq \frac{9}{4}$, our condition (33) on ε and (38) give

$$\dot{\tilde{V}}_o \;\leq\; -\tfrac{c}{10}\tilde{V}_o - \tfrac{81}{200}\kappa_1 m_1 \left|\tfrac{\partial \tilde{V}_o}{\partial e_2}(e_1,e_2)\right| + |\varepsilon y_d| \left|\tfrac{\partial \tilde{V}_o}{\partial e_2}(e_1,e_2)\right| \;\leq\; -\tfrac{c}{10}\tilde{V}_o. \tag{39}$$

2) $\lambda \left|\frac{\partial \tilde{V}_o}{\partial e_2}(e_1,e_2)\right| \leq \frac{9}{4}$. Then, since $|\sigma(r)| \geq \frac{r}{4}$ for $|r| \leq \frac{9}{4}$, the general relation $pq \leq \frac{9}{80}p^2 + \frac{20}{9}q^2$ and (38) give

$$\begin{aligned} \dot{\tilde{V}}_o &\leq -\tfrac{c}{10}\tilde{V}_o - \tfrac{9}{80}\kappa_1 m_1 \lambda \left|\tfrac{\partial \tilde{V}_o}{\partial e_2}(e_1,e_2)\right|^2 + |\varepsilon y_d| \left|\tfrac{\partial \tilde{V}_o}{\partial e_2}(e_1,e_2)\right| \\ &\leq -\tfrac{c}{10}\tilde{V}_o + \tfrac{20}{9\kappa_1 m_1 \lambda} y_d^2 \varepsilon^2. \end{aligned} \tag{40}$$

We deduce that, in both cases, we have

$$\dot{\tilde{V}}_o \;\leq\; -\tfrac{c}{10}\tilde{V}_o + \tfrac{20 y_d^2}{9\kappa_1 m_1 \lambda}\varepsilon^2 \tag{41}$$

along the trajectories of (35).

Using the relation $pq \leq \theta p^2/2 + q^2/\{2\theta\}$, with $p = 2|e_2| + B|e_1|$ and $q = \zeta^2 + 2|\zeta|\overline{R}$, and recalling our choice of $\overline{R}$ and the constants from (31) and (32), we can use (41) to get

$$\begin{aligned} \dot{\tilde{V}}_o &\leq -\tfrac{c}{10}\tilde{V}_o + \tfrac{20 y_d^2}{9\kappa_1 m_1 \lambda}\varepsilon^2 + \{2|e_2| + B|e_1|\}\{\zeta^2 + 2|\zeta|\overline{R}\} \\ &\leq -\tfrac{c}{20}\tilde{V}_o + \tfrac{1}{2\theta}\left[\zeta^2 + 2|\zeta|\overline{R}\right]^2 + \tfrac{20 y_d^2}{9\kappa_1 m_1 \lambda}\varepsilon^2 \;\leq\; -\tfrac{c}{20}\tilde{V}_o + M(\zeta^2 + \zeta^4) + \tfrac{20 y_d^2}{9\kappa_1 m_1 \lambda}\varepsilon^2 \end{aligned} \tag{42}$$

along the trajectories of (29). Next note that our choice (34) of μ gives $|\mu| \leq \frac{9}{20}\kappa_1 m_1 \lambda (2|e_2| + B|e_1|)$ and

$$\begin{aligned} \dot{\mu} \;=\; & -\tfrac{9}{20}\lambda\kappa_1 m_1 \sigma'(\lambda\{2e_2 + Be_1\})\left\{Be_2 + 2[-\kappa_1 e_1 - \kappa_2 e_2 + \mu(e_1,e_2)\right. \\ & \left. + \zeta^2 + 2\zeta R_\mu(e_1,e_2,t) - \varepsilon(e_1 + y_d)]\right\}. \end{aligned}$$

Since $|\varepsilon| \leq \kappa_2$, we readily conclude that $|\dot{\mu}| \leq \lambda^2 \tilde{\mathcal{L}}(|e_1| + |e_2| + \zeta^2 + |\zeta| + |\varepsilon|)$. Let $U(\zeta) = (M+1)\left(\zeta^4/4 + \zeta^2/2\right)$. We can use the general relation $pq \leq \frac{1}{4}p^2 + q^2$ and our lower bound on λ to get the time derivative

$$\begin{aligned} \dot{U} &\leq -\lambda^6(M+1)[\zeta^2 + \zeta^4 + \zeta^6] + \left\{\lambda^3(|\zeta|^3 + |\zeta|)\right\}\left\{\tfrac{|\dot{\mu}|(M+1)}{2R_\mu(e_1,e_2,t)\lambda^3}\right\} \\ &\leq -\tfrac{1}{2}\lambda^6(M+1)[\zeta^2 + \zeta^4 + \zeta^6] + (M+1)^2 \tfrac{\tilde{\mathcal{L}}^2(|e_1| + |e_2| + \zeta^2 + |\zeta| + |\varepsilon|)^2}{4\lambda^2 \underline{R}^2} \\ &\leq -\tfrac{1}{2}\lambda^6(M+1)[\zeta^2 + \zeta^4 + \zeta^6] + 2(M+1)^2 \tfrac{\tilde{\mathcal{L}}^2(e_1^2 + e_2^2 + \zeta^4 + \zeta^2 + \varepsilon^2)}{\lambda^2 \underline{R}^2} \\ &\leq -\tfrac{1}{4}\lambda^6(M+1)[\zeta^2 + \zeta^4 + \zeta^6] + \tfrac{c}{40}\tilde{V}_o + \tfrac{2(M+1)^2\tilde{\mathcal{L}}^2}{\lambda^2 \underline{R}^2}\varepsilon^2 \end{aligned} \tag{43}$$

along the trajectories of (29). Let $V = \tilde{V}_o + U$. Setting

$$\delta_1 = \min\left\{\frac{c}{40}, \frac{1}{1+M}\right\} \;\text{ and }\; \delta_2 = \frac{20 m_2^2}{9\kappa_1 m_1 \lambda} + \frac{2(M+1)^2\tilde{\mathcal{L}}^2}{\lambda^2 \underline{R}^2},$$

and combining (42) and (43) gives $\dot{V} \leq -\frac{c}{40}\tilde{V}_o + \delta_2\varepsilon^2 - (\zeta^4 + \zeta^2) \leq -\delta_1 V + \delta_2\varepsilon^2$. Integrating, this gives

$$V(Y(t)) \ \leq \ e^{-(t-t_o)\delta_1} V(Y(t_o)) + \frac{\delta_2}{\delta_1}\varepsilon^2 \tag{44}$$

along all trajectories $Y(t)$ of (29). Since

$$\min\{\omega_1, (M+1)/2\}\,|Y|^2 \leq V(Y) \leq \max\{\omega_2, (M+1)/2\}\,(|Y|^2 + |Y|^4)$$

everywhere, we can combine (44) and the general relation $\sqrt{r+s} \leq \sqrt{2r} + \sqrt{2s}$ for $r, s \geq 0$ to get

$$|Y(t)| \ \leq \ \sqrt{\frac{2e^{-(t-t_o)\delta_1}\max\left\{\omega_2, \frac{M+1}{2}\right\}}{\min\left\{\omega_1 \frac{M+1}{2}\right\}}(|Y(t_o)|^2 + |Y(t_o)|^4)} + |\varepsilon|\sqrt{\frac{2\delta_2}{\delta_1 \min\left\{\omega_1, \frac{M+1}{2}\right\}}}.$$

Since $\lambda > 0$ can be made as large as desired, the result follows. ∎

Remark 6. *The bound (33) leads to ISS with arbitrarily small linear overflows. If we merely want to prove ISS of the closed loop dynamics (29) with respect to ε (without regard to the particular choice of the overflow rate in the ISS estimate), then we can instead use the less stringent bound*

$$|\varepsilon| \leq \min\left\{\tfrac{9B\kappa_1}{20(B+1)}, \tfrac{9\kappa_2}{20}\right\}. \tag{45}$$

The proof of ISS with respect to uncertainties satisfying (45) proceeds as in the proof of Theorem 3 up through (38), at which point we can apply the general relation $pq \leq \delta p^2/2 + q^2/(2\delta)$ for a small enough constant $\delta > 0$ and the quadratic lower bound on $\tilde{V}_o$ to obtain a constant $\overline{\delta} > 0$ so that along the trajectories of (29),

$$\dot{\tilde{V}}_o \ \leq \ -\frac{c}{20}\tilde{V}_o + \{2|e_2| + B|e_1|\}\{\zeta^2 + 2|\zeta|\overline{R}\} + \overline{\delta}\varepsilon^2.$$

A slight variant of the argument used in (42) with a smaller choice of θ and a large enough constant $\lambda > 0$ then gives

$$\dot{\tilde{V}}_o \ \leq \ -\frac{c}{30}\tilde{V}_o + M(\zeta^2 + \zeta^4) + \overline{\delta}\varepsilon^2.$$

The remainder of the ISS proof closely follows the rest of the proof of Theorem 3. Our conclusion is that there exist $\beta \in \mathcal{KL}$ and a constant $\overline{\Delta} > 0$ such that for all of the closed loop trajectories $Y(t)$ of (29) with μ as in Theorem 3 and λ large enough, and for all initial times $t_o \geq 0$, we have $|Y(t)| \leq \beta(|Y(t_o)|, t - t_o) + \overline{\Delta}|\varepsilon|$ for all $t \geq t_o$, provided the uncertainty ε in (29) is constrained to satisfy the less stringent bound (45).

Remark 7. *Analogous results apply when the uncertainty is instead in the parameter b from (1). We model this situation by replacing b with $b + \varepsilon m$ in (1), where m is the movable electrode mass and the unknown constant ε represents the uncertainty. Changing variables as before, we get the transformed dynamics (29) except with $\varepsilon(e_1 + y_d)$ replaced by $\varepsilon(e_2 + \dot{y}_d)$. We then consider the corresponding reduced system*

$$\left\{\begin{array}{rcl} \dot{e}_1 &=& e_2 \\ \dot{e}_2 &=& -\kappa_1 e_1 - \kappa_2 e_2 + \mu(e_1, e_2) - \varepsilon(e_2 + \dot{y}_d) \end{array}\right. \tag{46}$$

and define $\tilde{V}_o$ in (30) as before. Let us now assume that the uncertainty satisfies

$$|\varepsilon| \leq \min\left\{\tfrac{\kappa_2}{5}, \tfrac{9\kappa_1}{20B}\right\}. \tag{47}$$

Then the relation $Be_1e_2 \leq B^2e_1^2 + \frac{1}{4}e_2^2$ gives

$$\left|\frac{\partial \tilde{V}_0}{\partial e_2}(e_1,e_2)\varepsilon e_2\right| \;\leq\; \left[B^2e_1^2 + \frac{9}{4}e_2^2\right]|\varepsilon| \;\leq\; \frac{9B\kappa_1}{20}e_1^2 + \frac{9\kappa_2}{20}e_2^2, \tag{48}$$

so the time derivative of $\tilde{V}_o$ along the trajectories of (46) satisfies

$$\dot{\tilde{V}}_o \leq -\frac{c}{10}\tilde{V}_o - \frac{9}{20}\kappa_1 m_1 \left|\frac{\partial \tilde{V}_o}{\partial e_2}(e_1,e_2)\right| \sigma\left(\lambda\left|\frac{\partial \tilde{V}_o}{\partial e_2}(e_1,e_2)\right|\right) + |\varepsilon \dot{y}_d|\left|\frac{\partial \tilde{V}_o}{\partial e_2}(e_1,e_2)\right|,$$

by arguing as in the proof of Theorem 3. The remainder of the ISS proof is as in Remark 6, using the fact that $|\varepsilon| \leq \kappa_2$ and a suitable choice of $\tilde{\mathcal{L}}$. Hence, the dynamics in closed loop with (34) are ISS with respect to uncertainties ε on $\kappa_2 = b/m$ that satisfy (47), provided the constant $\lambda > 0$ is large enough. Similar results hold when there are two independent (but suitably small) uncertainties, one on b and one on k. We leave the details to the reader.

7 Simulations

To demonstrate the efficacy of our methods, we simulated (1) in closed loop with the feedback u from (7), v_1 from (14), and μ given by (12). We took $a_1 = a_2 = 1$ and $a_3 = 100$. We used the model parameters $k = 2.5$, $m = 1$, $b = 1$, $\alpha = 0.5$, $\beta = 0.001$, $\gamma = 1$, and $g_o = 1$, and the C^3 periodic reference trajectory

$$\begin{aligned} y_d(t) &= 0.01 + \varepsilon_1\left[\mathcal{I}(500 + \min\{t, 50\}) - \mathcal{I}(\min\{\max\{t, 450\}, 550\})\right. \\ &\quad \left. +\mathcal{I}(\max\{t, 950\} - 500)\right] \;\text{ for }\; 0 \leq t \leq 1000, \\ y_d(t) &= y_d(t - 1000) \;\text{ for }\; t \geq 1000, \end{aligned} \tag{49}$$

where $\mathcal{I}(r) = \int_{450}^{r}(s-450)^3(550-s)^3 \mathrm{d}s$ and $\varepsilon_1 = .99/\mathcal{I}(550) = 1.386 \times 10^{-12}$. The function in (49) is a smoothed version of a standard square wave with a 0.01 offset; see Figure 2 below. This function mimics the periodic opening and closing of the relay. The conditions in (3) are satisfied with $m_1 = 0.01$, $m_2 = 1$, $m_3 = 0.0216$, and $m_4 = 0.00074386$, so $\underline{R} = 0.01249$ and $\overline{R} = \sqrt{5}$.

For the initial value $(x, \dot{x}, z)(0) = (0, 0, 10)$, we obtained the simulation in Figure 3 for the error $e_1(t) = x(t) - y_d(t)$. Figures 4-5 show the control signal u in its transient and steady states, respectively. Our simulation illustrates the rapid convergence of the tracking error to zero. The convergence also enjoys highly desirable robustness properties with respect to uncertainties on the parameters b and k. In this case, the bound in (45) is 0.45, so the convergence is ISS with respect to additive uncertainty ε on k, provided $|\varepsilon|$ is constrained to be below 18% of the nominal value $k = 2.5$. Moreover, the bound in (47) is 0.2, so the convergence is ISS with respect to uncertainties ε on b that stay below 20% of the nominal value $b = 1$.

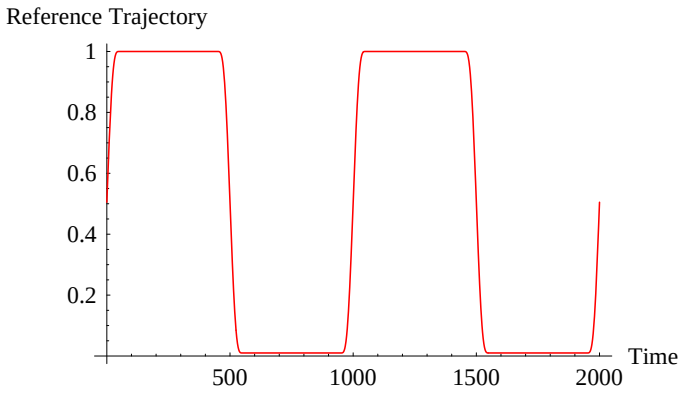

Figure 2: Smoothed Square Wave

8 Conclusions

In this paper, we designed a class of nonlinear tracking controllers for electrostatic and electromagnetic MEM relays. Explicit conditions on the reference trajectory were established, which were later shown to be compatible with the typical, alternating on-off operation of the relay. State and partial-state (i.e., no velocity measurement) feedbacks were constructed using Lyapunov theory. Further, ISS tools were used to quantify the robustness of the controls to parametric uncertainty. Although the structure of the relay dynamics prevents one from designing tracking control laws that yield global arbitrarily fast exponential convergence of the tracking error to zero, we showed that the proposed state feedback control enjoys this property locally. A numerical simulation illustrated the good tracking performance of the state feedback control for a smoothed periodic square wave, which mimics the repeated opening and closing of the relay.

References

[1] R.C. Anderson, B. Kawade, K. Ragulan, D.H.S. Maithripala, J.M. Berg, R.O. Gale, and W.P. Dayawansa, "Integrated Charge and Position Sensing for Feedback Control of Electrostatic MEMS," *Proc. SPIE Conf. Smart Structures and Materials*, San Diego, CA, 2005.

[2] J. Bergqvist, F. Rudolf, J. Maisano, F. Parodi, and M. Rossi, "A Silicon Condenser Microphone with a Highly Perforated Backplate," *Intl. Conf. Solid-State Sensors Actuators Digest*, pp. 266-269, New York, NY, 1991.

[3] B. Borovic, C. Hong, A.Q. Liu, L. Xie, and F.L. Lewis, "Control of a MEMS Optical Switch," *Proc. Conf. Decision and Control*, pp. 3039-3044, Paradise Island, Bahamas, 2004.

[4] I.J. Busch-Vishniac, "The Case for Magnetically Driven Microactuators," *Sensors and Actuators A*, No. 33, pp. 207-220, 1992.

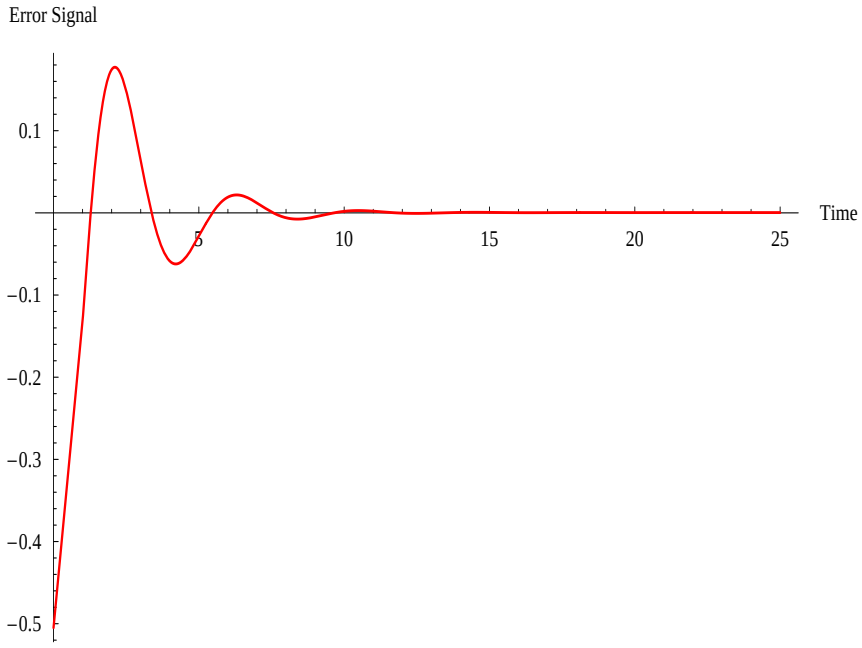

Figure 3: Error $e_1(t) = x(t) - y_d(t)$

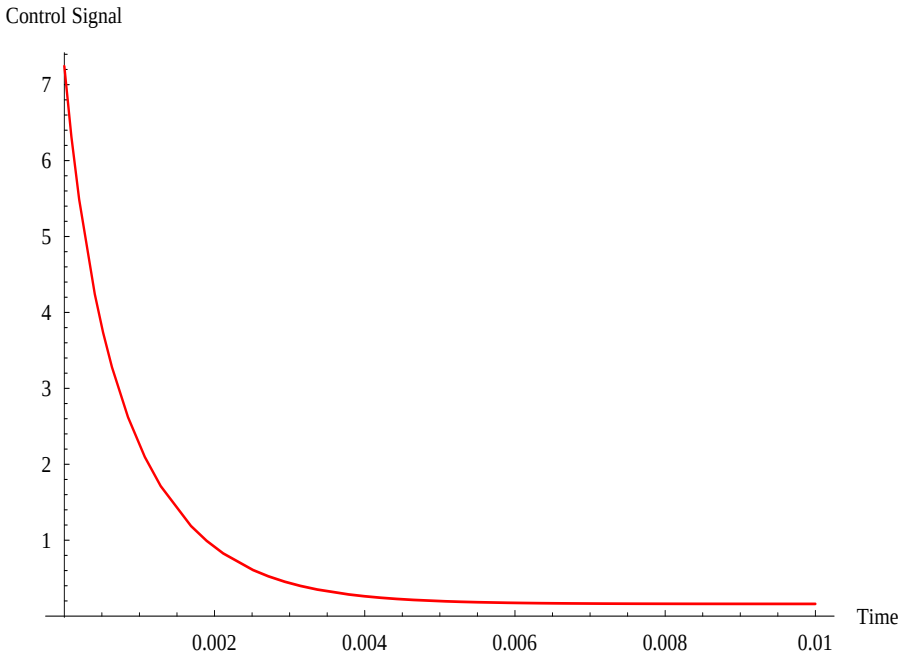

Figure 4: Control Signal u in Transient State

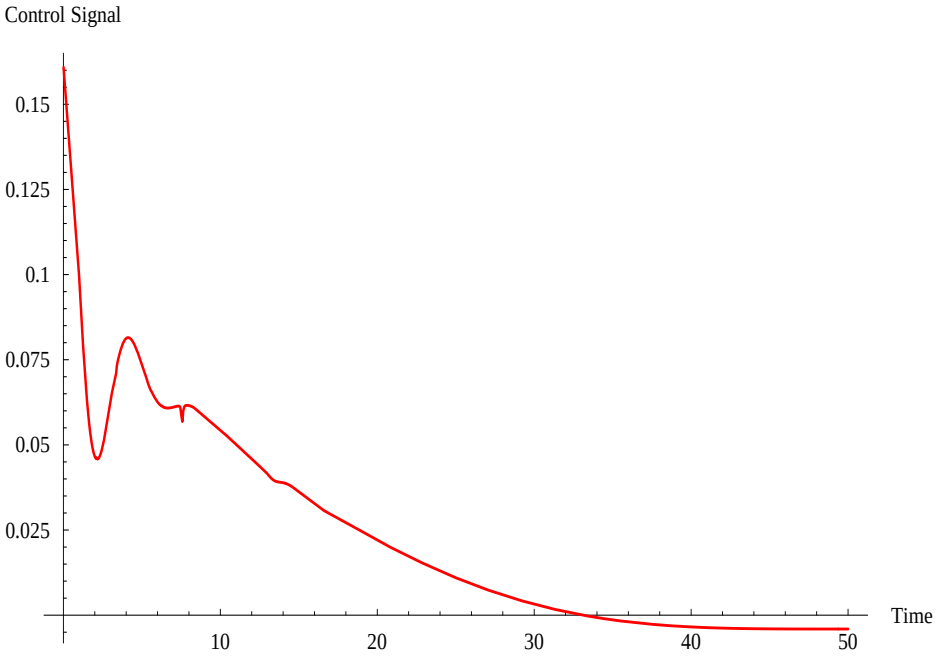

Figure 5: Control Signal u Approaching Steady State

[5] H. Guckel, T. Earles, J. Klein, J.D. Zook, and T. Ohnstein, "Electromagnetic Linear Actuators with Inductive Position Sensing," *Sensors and Actuators A*, No. 53, pp. 386-391, 1996.

[6] H. Hosaka, H. Kuwano, and K. Yanagisawa, "Electromagnetic Microrelays: Concepts and Fundamental Characteristics," *Sensors and Actuators A*, No. 40, pp. 41-47, 1994.

[7] S.J. Jeong, *UV-LIGA Micro-Fabrication of Inertia Type Electrostatic Transducers and Their Application*, Ph.D. Dissertation, Louisiana State University, 2005.

[8] H. Khalil, *Nonlinear Systems, Third Edition*, Englewood Cliffs, NJ: Prentice Hall, 2002.

[9] M. Krstic, I. Kanellakopoulos, and P. Kokotovic, *Nonlinear and Adaptive Control Design*, New York, NY: John Wiley & Sons, 1995.

[10] D.H.S. Maithripala, J.M. Berg, and W.P. Dayawansa, "Capacitive Stabilization of an Electrostatic Actuator: An Output Feedback Viewpoint," *Proc. American Control Conf.*, pp. 4053-4058, Denver, CO, 2003.

[11] D.H.S. Maithripala, J.M. Berg, and W.P. Dayawansa, "Control of an Electrostatic Microelectromechanical System Using Static and Dynamic Output Feedback," *ASME J. Dynamic Systems, Measurement, and Control*, Vol. 127, No. 3, pp. 443-450, 2005.

[12] D.H.S. Maithripala, B.D. Kawade, J.M. Berg, and W.P. Dayawansa, "A General Modelling and Control Framework for Electrostatically Actuated Mechanical Systems," *Intl. J. Robust and Nonlinear Control*, Vol. 15, pp. 839-857, 2005.

[13] B. McCarthy, G.G. Adams, N.E. McGruer, and D. Potter, "A Dynamic Model, Including Contact Bounce, of an Electrostatically Actuated Microswitch," *J. Microelectromechanical Systems*, Vol. 11, No. 3, pp. 276-283, 2002.

[14] R. Nadal-Guardia, A. Dehé, R. Aigner, and L.M. Castañer, "Current Drive Methods to Extend the Range of Travel of Electrostatic Microactuators Beyond the Voltage Pull-In Point," *J. Microelectromechanical Systems*, Vol. 11, No. 3, pp. 255-263, 2002.

[15] S.D. Senturia, *Microsystem Design*, New York, NY: Springer, 2004.

[16] E.D. Sontag, "Smooth Stabilization Implies Coprime Factorization," *IEEE Transactions on Automatic Control*, Vol. 34, No. 4, pp. 435-443, 1989.

[17] E.D. Sontag, "Input-to-State Stability: Basic Concepts and Results," in *Nonlinear and Optimal Control Theory*, Berlin, Germany: Springer, 2006, pp. 163-220.

[18] J.D. Williams, *Design and Fabrication of Electromagnetic Micro-Relays Using the UV-LIGA Technique*, Ph.D. Dissertation, Louisiana State University, 2004.

[19] M. Younis, F. Gao, and M.S. de Queiroz, "A Generalized Approach for the Control of MEM Relays," *Proc. American Control Conf.*, New York, NY, July 2007, to appear.

[20] G. Zhu, J. Lévine, and L. Praly, "Improving the Peformance of an Electrostatically Actuated MEMS by Nonlinear Control: Advances and Comparison," *Proc. Conf. Decision and Control*, pp. 7534-7539, Seville, Spain, 2005.

[21] G. Zhu, J. Penet, and L. Saydy, "Robust Control of an Electrostatically Actuated MEMS in the Presence of Parasitics and Parameter Uncertainties," *Proc. American Control Conf.*, pp. 1233-1238, Minneapolis, MN, 2006.